# The Green Function Approach to the Two-Dimensional $t-J$ model *

SONG Bo(宋波)[1,2,3], WANG Yu-Peng(王玉鹏)[2]

[1] *Technical Institute of Physics and Chemistry, Chinese Academy of Sciences, Beijing 100080*
[2] *Institute of Physics and Center for Condensed Matter Physics, Chinese Academy of Sciences, Beijing 100080*
[3] *Graduate School, Chinese Academy of Sciences, Beijing 100039*

(Received 21 November 2002)

*We investigate the two-dimensional $t-J$ model by the Green function approach with the Hubbard operator. The phase diagram, including the Neel temperature and the superconducting transition temperature simultaneously, is derived. The results are consistent with experiments of cuprate compounds.*

*PACS: 74.72.−h, 74.25.−q, 74.25.Dw*

The discovery of the high-$T_c$ superconductivity in cuprates[1] has stimulated strong experimental and theoretical interests in mechanisms of superconductivity. Experimental results indicate that the following properties are essential. Firstly, the $CuO_2$ layered structure is intrinsic to superconductivity and both of the undoped and carrier doped $CuO_2$ planes are characterized as a two-dimensional system from its magnetic,[2] transport,[3] and optical properties.[4] Secondly, superconductivity occurs in a disordered spin background.[5] For the undoped case, the system is a Mott insulator and spins at Cu sites show antiferromagnetic (AF) long-range order below the Neel temperature $T_{\rm N}$. For the doping case, $T_{\rm N}$ decreases to zero and spin-glass behaviour is observed.[6] Superconductivity emerges with the further doping. Apparently disorder in the spin system is due to doped holes. Thirdly, the Cooper pairs exhibit d-wave symmetry.[7]

Anderson suggested that the large-U limit of the Hubbard model is related to high-$T_{\rm C}$ superconductivity in cuprates.[5] It is well known that the Hubbard model in the large-U limit is equivalent to the so-called $t-J$ model.[8,9] Many investigations on this model have used the slave-boson approach in mean-field theory.[10−12] This approach is based on spin-charge separation in two dimensions (2D). The basic idea is that there are three kinds of excitations of the resonating valence bond (RVB) states. The first is fermion spin soliton (spinon). The second is boson–hole with charge (holon). The third is an electron or a hole, which is the product of the above two. The spin-charge correlation between the holon and the spinon is sufficiently weak for spin-charge separation.[13,14] By this method, the superconducting (SC) phase is stable for heavy hole doping, i.e., large $\delta$, which coincides with experimental results. However, in small $\delta$ region, the method yields the results that are not consistent with experimental results.

In this Letter, we consider the $t-J$ model in a square lattice. Instead of assuming spin-charge separation, we investigate the $t-J$ model with the Hubbard operator[8] directly. By the Green function method in mean-field theory, we obtain the phase diagram and discuss the AF order and the SC order simultaneously.

The model Hamiltonian reads

$$\begin{aligned} H =& -t\sum_{\langle i_A,i_B\rangle,\sigma} P(C^{\dagger}_{i_A,\sigma}C_{i_B,\sigma}+C^{\dagger}_{i_B,\sigma}C_{i_A,\sigma})P \\ &+J\sum_{\langle i_A,i_B\rangle}(\boldsymbol{S}_{i_A}\cdot\boldsymbol{S}_{i_B}-\frac{1}{4}n_{i_A}n_{i_B}) \\ &-\mu_0\Big[\sum_{i_A,\sigma}C^{\dagger}_{i_A,\sigma}C_{i_A,\sigma}+\sum_{i_B,\sigma}C^{\dagger}_{i_B,\sigma}C_{i_B,\sigma}\Big], \end{aligned} \tag{1}$$

where $i_A$ and $i_B$ label the sublattices $A$ and $B$ respectively, which are introduced for investigating the AF order; $\langle i_A,i_B\rangle$ means the nearest neighbour; $t$ is the hopping constant and $J>0$ is the AF coupling constant of electron spins; $P\cdots P$ represents the single occupation condition $n_{i_A}=\sum_\sigma C^{\dagger}_{i_A,\sigma}C_{i_A,\sigma}\le 1$; $C^{\dagger}_{i_A,\sigma}$ ($C^{\dagger}_{i_B,\sigma}$) represents the creation operator of electrons on site $i_A$ ($i_B$), $C_{i_A,\sigma}$ ($C_{i_B,\sigma}$) means the annihilation operator of electrons on site $i_A$ ($i_B$); $\boldsymbol{S}_{i_A}$ ($\boldsymbol{S}_{i_B}$) denotes the spin operator of electron on site $i_A$ ($i_B$); $\mu_0$ is the chemical potential; $i_A$ and $i_B$ run through the sublattices $A$ and $B$, respectively.

We introduce the SC order parameter in the form of

$$\Delta=\langle C_{i_B,\downarrow}C_{i_A,\uparrow}-C_{i_B,\uparrow}C_{i_A,\downarrow}\rangle. \tag{2}$$

Because we have divided the lattice into sublattices $A$ and $B$, the AF order parameters can be introduced as follows:

$$\begin{aligned} M =& \langle C^{\dagger}_{i_A,\uparrow}C_{i_A,\uparrow}-C^{\dagger}_{i_A,\downarrow}C_{i_A,\downarrow}\rangle \\ =& -\langle C^{\dagger}_{i_B,\uparrow}C_{i_B,\uparrow}-C^{\dagger}_{i_B,\downarrow}C_{i_B,\downarrow}\rangle. \end{aligned} \tag{3}$$

In addition, we assume $\langle n_{B,\sigma}\rangle=\langle n_{A,\bar\sigma}\rangle$. With the order parameters defined above, using the Green function and cut-off techniques,[15] we obtain the Green

* Supported by the National Natural Science Foundation of China under Grant No 90103024.
©2003 Chinese Physical Society and IOP Publishing Ltd

functions and the energy spectrum of the system as follows:

$$\begin{aligned}&\langle\langle C^A_{k,\sigma}; C^{A\dagger}_{k,\sigma}\rangle\rangle\\ =&\frac{1-n_{\bar\sigma}}{(\omega+E_+)(\omega-E_+)(\omega+E_-)(\omega-E_-)}\\ &\cdot\{\omega^3-\mu_{\bar\sigma}\omega^2-(\mu^2_\sigma+\epsilon_{k,\sigma}\epsilon_{k,\bar\sigma}+|\Delta_k|^2)\omega\\ &+(\mu^2_\sigma\mu_{\bar\sigma}-\mu_\sigma\epsilon_{k,\sigma}\epsilon_{k,\bar\sigma}+\mu_{\bar\sigma}|\Delta_k|^2)\},\end{aligned}\tag{4}$$

$$\begin{aligned}&\langle\langle C^B_{k,\sigma}; C^{A\dagger}_{k,\sigma}\rangle\rangle\\ =&\frac{(1-n_{\bar\sigma})\epsilon_{k,\sigma}}{(\omega+E_+)(\omega-E_+)(\omega+E_-)(\omega-E_-)}\\ &\cdot\{\omega^2-2\mu\omega+(\mu_\sigma\mu_{\bar\sigma}-\epsilon_{k,\sigma}\epsilon_{k,\bar\sigma}-\frac{\epsilon_{k,\bar\sigma}}{\epsilon_{k,\sigma}}|\Delta|^2)\},\end{aligned}\tag{5}$$

$$\begin{aligned}&\langle\langle C^{B\dagger}_{\bar k,\bar\sigma}; C^{A\dagger}_{k,\sigma}\rangle\rangle\\ =&-\frac{(1-n_{\bar\sigma})\Delta^*_k}{(\omega+E_+)(\omega-E_+)(\omega+E_-)(\omega-E_-)}\\ &\cdot\{\omega^2-(\epsilon^2_{k,\sigma}+\mu^2_\sigma+|\Delta_k|^2)\},\end{aligned}\tag{6}$$

and

$$E_\pm(k)=\sqrt{\frac{1}{2}(\mu^2_\uparrow+\mu^2_\downarrow)+\epsilon_{k,\uparrow}\epsilon_{k,\downarrow}+|\Delta_k|^2\pm D},\tag{7}$$

with

$$D=\sqrt{4J^{*2}M^2\mu^2+4\mu^2\epsilon_{k,\uparrow}\epsilon_{k,\downarrow}-(\epsilon_{k,\uparrow}-\epsilon_{k,\downarrow})^2|\Delta_k|^2},\tag{8}$$

$$\epsilon_{k,\sigma}=-\delta t\gamma_k-K_{k,\sigma},\tag{9}$$

$$K_{k,\sigma}=J^*[K_{x,\sigma}\cos(k_xa)+K_{y,\sigma}\cos(k_ya)],\tag{10}$$

$$\Delta_k=3J^*[\Delta_x\cos(k_xa)+\Delta_y\cos(k_ya)],\tag{11}$$

$$K_\sigma=\langle C^\dagger_{i_B,\sigma}C_{i_A,\sigma}\rangle,\tag{12}$$

$$\mu_\uparrow=\mu-J^*M,\tag{13}$$

$$\mu_\downarrow=\mu+J^*M,\tag{14}$$

$$\mu=\mu_0+J^*(n_\uparrow+n_\downarrow),\tag{15}$$

$$\gamma_k=2\cos(k_xa)+2\cos(k_ya),\tag{16}$$

$$n_\sigma=n_{A,\sigma},\tag{17}$$

$$J^*=\frac{1}{4}J.\tag{18}$$

Then, we can obtain the free energy of system from the equation:

$$F=\frac{1}{\beta}\int_0^\beta\langle H\rangle d\beta.\tag{19}$$

The phases of parameters $K_x$, $K_y$ and $\Delta_x$, $\Delta_y$ in Eqs. (10) and (11) are introduced as follows:

$$K_y=K_x\exp(\mathrm{i}\alpha),\quad \Delta_y=\Delta_x\exp(\mathrm{i}\beta).\tag{20}$$

By minimizing the free energy, we can determine $\alpha=0$ and $\beta=\pi$. Thus we can see that Cooper pairs show the d-wave symmetry.

With spectral function,[15] we obtain the self-consistent equations of the mean-field order parameters $\Delta_x$, $K_\uparrow$, $K_\downarrow$, and $M$:

$$\begin{aligned}1-\delta=&\frac{1}{2}(1+\delta)+\sum_k\frac{1}{2(E^2_+-E^2_-)}\\ &\cdot\Big\{\frac{2J^*\mu[\mu+J^*(1+\delta)]M^2}{E_+}\tanh\frac{\beta E_+}{2}\\ &+\frac{(\epsilon_{k,\uparrow}\epsilon_{k,\downarrow})2\mu(1+\delta)}{E_+}\tanh\frac{\beta E_+}{2}\\ &+\frac{[(1+\delta)\mu+J^*M^2]D}{E_+}\tanh\frac{\beta E_+}{2}\\ &-\frac{2J^*\mu[\mu+J^*(1+\delta)]M^2}{E_-}\tanh\frac{\beta E_-}{2}\\ &-\frac{(\epsilon_{k,\uparrow}\epsilon_{k,\downarrow})2\mu(1+\delta)}{E_-}\tanh\frac{\beta E_-}{2}\\ &+\frac{[(1+\delta)\mu+J^*M^2]D}{E_-}\tanh\frac{\beta E_-}{2}\Big\},\end{aligned}\tag{21}$$

$$\begin{aligned}M=&\frac{1}{2}M+\sum_k\frac{M}{2(E^2_+-E^2_-)}\\ &\cdot\Big\{\frac{2J^*\mu[(1+\delta)\mu+J^*M^2]+2(\epsilon_{k,\uparrow}\epsilon_{k,\downarrow})\mu}{E_+}\\ &\cdot\tanh\frac{\beta E_+}{2}+\frac{[\mu+J^*(1+\delta)]D}{E_+}\tanh\frac{\beta E_+}{2}\\ &-\frac{2J^*\mu[(1+\delta)\mu+J^*M^2]+2(\epsilon_{k,\uparrow}\epsilon_{k,\downarrow})\mu}{E_-}\\ &\cdot\tanh\frac{\beta E_-}{2}+\frac{[\mu+J^*(1+\delta)]D}{E_-}\tanh\frac{\beta E_-}{2}\Big\},\end{aligned}\tag{22}$$

$$\begin{aligned}K_\uparrow=&\sum_k\frac{\epsilon_{k,\uparrow}\gamma_k(1-n_\downarrow)}{8(E^2_+-E^2_-)}\\ &\cdot\Big\{\frac{2\mu^2+\Big(1-\dfrac{\epsilon_{k,\downarrow}}{\epsilon_{k,\uparrow}}\Big)|\Delta_k|^2+D}{E_+}\tanh\frac{\beta E_+}{2}\\ &-\frac{2\mu^2+\Big(1-\dfrac{\epsilon_{k,\downarrow}}{\epsilon_{k,\uparrow}}\Big)|\Delta_k|^2-D}{E_-}\tanh\frac{\beta E_-}{2}\Big\},\end{aligned}\tag{23}$$

$$\begin{aligned}K_\downarrow=&\sum_k\frac{\epsilon_{k,\downarrow}\gamma_k(1-n_\uparrow)}{8(E^2_+-E^2_-)}\\ &\cdot\Big\{\frac{2\mu^2+\Big(1-\dfrac{\epsilon_{k,\uparrow}}{\epsilon_{k,\downarrow}}\Big)|\Delta_k|^2+D}{E_+}\tanh\frac{\beta E_+}{2}\\ &-\frac{2\mu^2+\Big(1-\dfrac{\epsilon_{k,\uparrow}}{\epsilon_{k,\downarrow}}\Big)|\Delta_k|^2-D}{E_-}\tanh\frac{\beta E_-}{2}\Big\},\end{aligned}\tag{24}$$

$$\Delta^*_x=\frac{3J^*\Delta^*_x}{16}\sum_k\frac{g^2_k}{E^2_+-E^2_-}$$

$$\cdot \Big\{ \frac{2J^*\mu M^2 + (1+\delta)D}{E_+} \tanh \frac{\beta E_+}{2} + \frac{\sum_\sigma (1-n_{\bar\sigma})(\epsilon_{k,\sigma}\epsilon_{k,\bar\sigma} - \epsilon^2_{k,\sigma})}{E_+} \tanh \frac{\beta E_+}{2} - \frac{2J^*\mu M^2 - (1+\delta)D}{E_-} \tanh \frac{\beta E_-}{2} - \frac{\sum_\sigma (1-n_{\bar\sigma})(\epsilon_{k,\sigma}\epsilon_{k,\bar\sigma} - \epsilon^2_{k,\sigma})}{E_-} \tanh \frac{\beta E_-}{2} \Big\}, \tag{25}$$

where $g_k = 2\cos(k_x a) - 2\cos(k_y a)$.

Taking $|\Delta_k| = 0$, from Eqs. (21)–(25), we can obtain the critical temperature of the SC order $T_{\rm C}$, chemical potential $\mu$, $K_{AB}$ and $M$. Similarly, taking $M = 0$, we can obtain the critical temperature $T_{\rm N}$ of the AF order, $\mu$, $K_{AB}$ and $|\Delta_x|$.

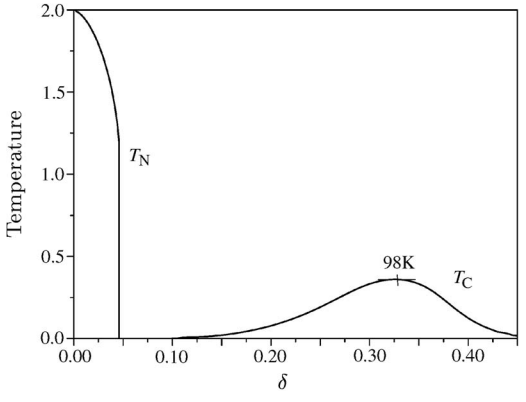



**Fig. 1.** Phase diagram at $t = 2.5J$. $T_{\rm N}$: Neel temperature, $T_{\rm C}$: critical temperature of the SC order, $|\delta|$: doping of holes.

For calculation, we take $J$ as energy unit. $T_{\rm N}$ and $T_{\rm C}$ with respect to the doping of holes $\delta$ are obtained as shown in Fig. 1.

The numerical results show that for $t = 2.5J$, the AF order is stable only for small $\delta$, while the SC order is stable for intermediate $\delta$. The AF order and the SC order do not coexist. In the region of the SC order, $T_{\rm C}$ has a maximum, $T_{\rm C,max} \cong 98\,{\rm K}$ if we take $J = 0.17\,{\rm eV}$ according to $La_2CuO$.[16] From Eq. (20), we can see that Cooper pairs show the d-wave symmetry. All of these features we have derived by the numerical methods are consistent with the experimental results for cuprate compounds.[1] Hopping holes easily destroy the AF order. Thus for large $t$, the AF order can be stable only for small $\delta$ region. For the SC order, in the over-doping region, the effect of electron hopping is strong so that Cooper pairs are easily destroyed. Electron hopping breaks down the SC order when $\delta$ is large. In the under-doping region, the hopping of Copper pairs weaken with decreasing $\delta$, which can prevent from condensation of Copper pairs. Thus in contrast to the experimental results, this method does not shows the SC order in the range of very small $\delta$ region (such as $\delta < 0.1$).

In summary, the 2D $t - J$ model is studied by the Green function technique with the cutoff theory. The advantage of this approach exhibits that we can use the hard-core fermion operator directly and can avoid to use the slave bosons. The phase diagram, including the Neel temperature and the SC transition temperature, which are consistent with experiments, are derived simultaneously.

# References


[1] Bednorz J G and Muller K A 1986 *Z. Phys.* B **64** 189
[2] Shirane G et al 1994 *Physica* B **197** 158
[3] Ito T et al 1991 *Nature* **350** 1196
[4] Homes C C et al 1993 *Phys. Rev. Lett.* **71** 1645
[5] Anderson P W 1987 *Science* **235** 1196
[6] Chou F C et al 1995 *Phys. Rev. Lett.* **75** 2204
[7] Scalapino D J 1995 *Phys. Rep.* **250** 329
[8] Koshibae W et al 1993 *Phys. Rev.* B **47** 3391
[9] Ye J et al 1999 *Phys. Rev. Lett.* **83** 3737
[10] Hirsh E 1985 *Phys. Rev. Lett.* **54** 1317
[11] Gros C, Joynt R and Rice T M 1987 *Phys. Rev.* B **36** 8190
[12] Kotliar G et al 1988 *Phys. Rev.* B **38** 5142
[13] Kivelson S A et al 1987 *Phys. Rev.* B **35** 8865
[14] Anderson P W et al 1987 *Phys. Rev. Lett.* **58** 2790
[15] Mahan G D 1990 *Many-Particle Physics* (New York: Plenum)
[16] Hybertsen M S, Stechel E B, Foulkes W M C and Schluter M 1992 *Phys. Rev.* B **45** 10032